Available online at www.sciencedirect.com
ScienceDirect
C. R. Physique 7 (2006) 622–633
COMPTES RENDUS PHYSIQUE
http://france.elsevier.com/direct/COMREN/

Turbulent transport in fusion magnetised plasmas/Transport turbulent dans les plasmas magnétisés de fusion

Physics of Internal Transport Barriers

Tuomas Tala [a], Xavier Garbet [b,*],

JET EFDA contributors [1]

[a] *Association EURATOM–TEKES, VTT, P.O. Box 1000, FIN-02044 VTT, Finland*
[b] *Association EURATOM–CEA, CEA Cadarache, 13108 St Paul-Lez-Durance, France*

Available online 17 August 2006

Abstract

This article presents an overview of the studies carried out at JET to clarify the physics of Internal Transport Barriers. Results of dedicated experiments, modelling and theory are reported. Several issues are discussed, namely the question of the dominant mechanisms for barrier formation and the nature of the transition, the role of magnetic surfaces in barrier triggering, the question of radial location and width of barriers, and the predictive capability of transport and turbulence modelling. ***To cite this article: T. Tala et al., C. R. Physique 7 (2006).***

Résumé

La physique des barrières internes de transport. Ce papier présente une synthèse des études menées sur le tokamak JET afin de clarifier la physique des barrières internes de transport. Les résultats expérimentaux, de modélisation et de théorie sont revus. Plusieurs points sont discutés, notamment la question des mécanismes en jeu pour la formation des barrières et la nature de la transition, le rôle du cisaillement magnétique, la position et la largeur des barrières, et le pouvoir de prédiction des modèles de transport turbulent. ***Pour citer cet article : T. Tala et al., C. R. Physique 7 (2006).***

Keywords: Plasma fusion; JET; Internal Transport Barriers

Mots-clés : Fusion de plasmas ; JET ; Barrières internes de transport

1. Introduction

Since the first observations of 'Internal Transport Barriers' (ITBs) in tokamaks [1–6], a tremendous effort has been undertaken to understand the underlying physics. There already exist several overviews addressing the physics of ITBs (see, for instance, [7,8]). The present paper focuses on specific issues related to the onset and sustainment of barriers, mainly illustrated by results obtained on the JET tokamak. Internal transport barriers can be defined as regions of the core plasma where turbulent transport is reduced or quenched. At given fluxes, the reduction of diffusion coefficients

* Corresponding author.
E-mail addresses: tuomas.tala@vtt.fi (T. Tala), garbet@cea.fr (X. Garbet).
[1] See the Appendix of J. Pamela et al., in: Fusion Energy, Proc. 20th Int. Conf. Vilamoura, 2004, IAEA, Vienna, 2004.

1631-0705/$ – see front matter
doi:10.1016/j.crhy.2006.06.005

leads to a local steepening of profiles. The triggering and sustainment of ITBs are complex issues and are known to depend on a large number of factors. However it is widely admitted that two ingredients play an important role in the dynamics of ITBs: the magnetic shear and the flow shear. Other mechanisms exist, which are less generic, and will not be detailed here. In spite of considerable progress, several issues need to be resolved.

The first issue deals with the relative role of magnetic shear and flow shear. The analysis of the JET database indicates that the amount of flow shear needed to trigger an ITB depends on the magnetic shear. Thus both quantities seem to be involved. On the other hand, pure electron barriers are characterised by a small mean flow shear. Hence the magnetic shear alone is able to produce an electron transport barrier. This question of interplay between flow shear and magnetic shear is related to the nature of the transition. In a 'first order' transition, a jump of temperature gradient takes place. This transition usually occurs above a critical heat flux, i.e., a heating power threshold. Also a hysteresis effect is expected in this case, i.e., the power below which the plasma moves back to low confinement (backward transition) is lower than the critical value for barrier formation. In a 'second order' transition, the temperature gradient is continuous at the threshold. In principle neither power threshold nor hysteresis are expected in this case. Of course reality is more complex as some heating power is always needed to reach the right conditions for a transition. Still this classification is quite useful and the understanding of the mechanisms that underlie the transition is certainly a central issue. However, an analysis of the JET database cannot remove the ambiguity on the nature of the transition. It turns out that heat modulation experiments provide a powerful tool to investigate this point.

A related open issue is the role of magnetic surfaces associated with low order rational values of the minimum safety factor. Experiments on JET have clearly shown that these surfaces often play an important role when a barrier is being formed. This puzzling behaviour raises a fundamental difficulty, as most theoretical models do not predict a special role of these surfaces. This question may be related to another surprising observation, namely values of the poloidal flow well above values predicted by neoclassical theory.

Another set of issues is related to the location and width of the barrier. Does the barrier appear at zero or negative magnetic shear? Does a barrier cover the whole central region, or does it exhibit a finite radial width? Again the database provides some elements of response, but error bars do not allow a definitive answer. Turbulence measurements and heat modulations experiments have provided invaluable information, although somewhat contradictory at first sight.

The interpretation and preparation of future experiments, but also the extrapolation of the present performances to next step devices such as ITER, require the development and validation of accurate modelling tools, ranging from 1D transport predictive modelling to 5D kinetic turbulence simulations. The JET profile database, which covers a large variety of steady and transient regimes, has been used extensively to test these models. Again dedicated experiments have proved their usefulness as their analysis requests usually a deeper exploration of the model capabilities.

The article is organised as follows. General considerations on ITB formation and sustainment are presented in Section 2. Dedicated experiments to understand the physics of ITBs are presented in Section 3. Predictive modelling and turbulence simulations are reviewed in Section 4. A conclusion follows in Section 5.

2. General considerations on barrier formation and sustainment

2.1. Micro-stability

The explanation for the triggering and sustainment of Internal Transport Barriers is usually based on a mixture of linear stabilisation and turbulence quench due to flow shear stabilisation.

The local magnetic shear is often considered as the main reason for improved stability. It is reminded here that the magnetic shear is related to the derivative of the safety factor. The latter is defined as the winding number of helical fields line on a magnetic surface (in other words $q = \mathbf{B} \cdot \nabla\varphi / \mathbf{B} \cdot \nabla\theta$, where φ and θ are the toroidal and poloidal angles). Hence the magnetic shear measures the variation of the field lines angle from one magnetic surface to an adjacent one. Two mechanisms have been identified for magnetic shear stabilisation. First, the growth rates of linear turbulent modes get smaller when the magnetic shear decreases. Interchange-like modes become ultimately stable at negative magnetic shear [9]. What counts is the local magnetic shear, which depends on the Shafranov shift of magnetic surfaces (defined as the difference between the centre of the last magnetic flux surface and that of the magnetic flux surface at a given ρ) [10]. A simple rule states that the local magnetic shear on the low field side is of the order of $s - \alpha$, where $s = r\,\mathrm{d}q/q\,\mathrm{d}r$ (q is the safety factor) and $\alpha = -q^2 R\,\mathrm{d}\beta/\mathrm{d}r$ measures the shift of

magnetic surfaces (β is the ratio of kinetic to magnetic pressures). Increasing α is equivalent to lowering s (hence the name 'α-stabilisation'). Second, a rarefaction of resonant surfaces occurs at zero magnetic shear and may lead to stabilisation [11]. Resonant surfaces are magnetic surfaces such that the associated safety factor is a rational number m/n. Modes with a poloidal and toroidal wave number m and n (i.e., which behave as $\exp[\mathrm{i}(m\theta + n\varphi)]$) are spatially localised close to the corresponding m, n resonant surface (when it exists). These 'resonant' modes are believed to play a prominent role in turbulence. It is well known that close to a low order rational number (e.g., $q = 2$), there exists an interval without rational numbers m/n if m and n are upper bounded. This constraint comes from linear stability: the range of relevant unstable wave numbers is finite. If resonant modes are important, a decrease of the level of fluctuations should occur in this region. However, this mechanism is subject to controversy, as it requires very low values of the toroidal wave numbers to be effective [12]. Also it was found in non linear kinetic simulations that non resonant modes fill the gap [13].

Flow shear stabilisation results from vortex distortion by the flow. It is reminded here that in a magnetised plasma, an electric field induces an electric drift velocity $\mathbf{V_E}$ that is perpendicular to both the magnetic field $\mathbf{B}$ and the electric field $\mathbf{E}$, i.e., $\mathbf{V_E} = \mathbf{E} \times \mathbf{B}/B^2$. The mean '$E \times B$ drift' varies radially in a tokamak, and may quench turbulence if its shear rate is high enough. A common way to assess the overall stability is to compare the $E \times B$ shear rate $\gamma_E = \mathrm{d}V_E/\mathrm{d}r$ to a maximum linear growth rate γ_{lin}, calculated without flow shear effects [14–16]. Full stabilisation is considered to be reached when $\gamma_E > \gamma_{\mathrm{lin}}$. This simple criterion has been widely used to assess the formation of barriers. In particular, operational criteria can be built on the basis of this simple rule [17,18].

Usually a minimum heating power is needed to trigger an ITB. Predicting this power threshold is not an easy task. The ITBs can be formed in a variety of plasma conditions. They can appear at various plasma radii, on various plasma profiles at various plasma power levels, with various plasma heating systems, different q-profiles, etc. [19]. For example, JET experiments with monotonic q-profile (positive magnetic shear) indicated that the power threshold needed to form an ITB increases with increasing toroidal magnetic field B_t [19,20]. However, this scaling dependence on B_t disappears if the q-profile is tailored, for example with lower hybrid current drive, to be reversed (negative magnetic shear). Consequently, it is unlikely that a universal power threshold based on global ('engineer') parameters can be found for ITB formation. In fact, ITB formation is clearly linked to the local values of parameters like magnetic shear, q-profile, $E \times B$ velocity shear. A striking observation on JET is that the transition often takes place when the minimum value of the safety factor q_{min} is a low order rational number, i.e., $q_{\mathrm{min}} = m_0/n_0$, where m_0 and n_0 are small integers (typically $q_{\mathrm{min}} = 2, 3/2, 3, \ldots$) [20,21]. Very recently, it is reported that actually the triggering event of the ITB occurs just before, typically 50–100 ms, q_{min} reaching the rational surface m_0/n_0 [22]. This phenomenon is shown with the Alfven cascades in the MHD spectrogram. This behaviour was also observed on DIII-D in some cases [23].

2.2. Local stability analysis

A detailed analysis of barrier formation can be done by using the criterion $\gamma_E > \gamma_{\mathrm{lin}}$. Several fluid and kinetic stability codes are currently used at JET to calculate the growth rates of linear micro-instabilities, mainly Ion Temperature Gradient (ITG) modes and Trapped Electron Modes (TEMs) [24–27] and the flow shearing rate [28–31]. The poloidal rotation velocity for the evaluation of the $E \times B$ velocity shear is calculated with the NCLASS code [32], or by using the analytical expression proposed by Kim et al. [33]. An example is given in Fig. 1 where these models are compared on the JET pulse #51976 (details can be found in [34]).

Most models do predict stabilisation, due to negative (or weak) magnetic shear and/or the Shafranov shift to trigger the barrier. In this case with negative magnetic shear inside $R = 3.4$ m, the Weiland model predicts a growth rate that remains larger than the flow shear rate.

The JET database has been analysed using a systematic stability analysis. A linear empirical threshold condition $\gamma_E/\gamma_{\mathrm{ITG}} > 0.68s - 0.095$ has been found for the onset of the ion internal transport barriers using the JET positive magnetic shear ITB database [35]. Here, s is the magnetic shear, γ_E is the flow shearing rate and γ_{ITG} is an approximate value of the linear growth rate of the ion temperature gradient instability. This empirical threshold condition for the ITB formation provides a clear indication of the strong correlation of the magnetic shear and the $E \times B$ flow shearing rate when the ITB forms. This empirical threshold condition is illustrated in Fig. 2. The trend to need larger γ_E shearing rates with increasing magnetic shear (at least up to $s \leqslant 1$) is consistent with other similar works [36,37]. This empirical threshold condition does not reveal whether a separate trigger, like a rational surface of q is needed

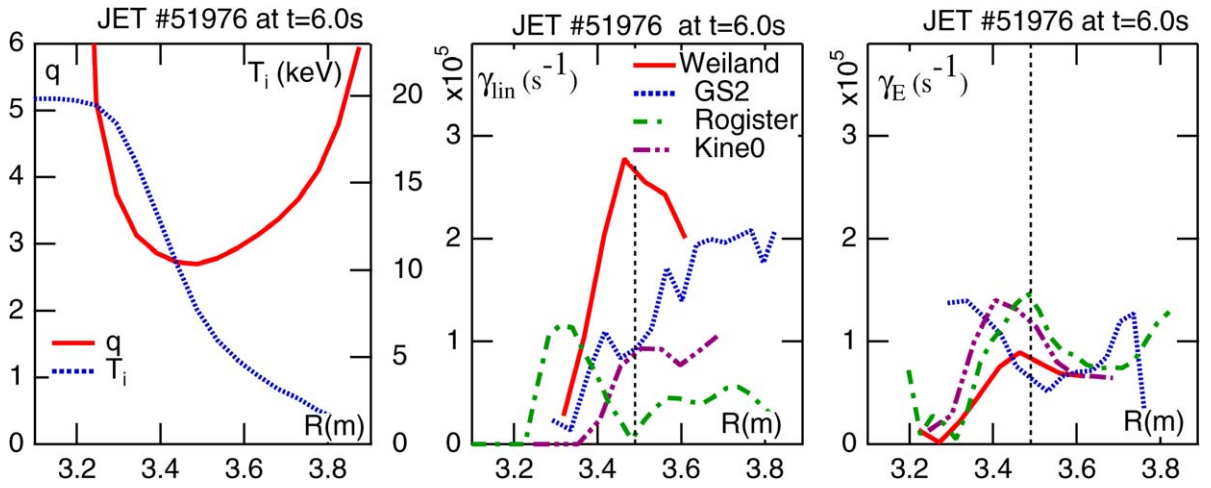

Fig. 1. Profiles of safety factor and ion temperature, linear growth rates and velocity shear rate of JET pulse #51976 at $t = 6$ s. The vertical line shows the radial footpoint of the ITB (reproduced from [34]).

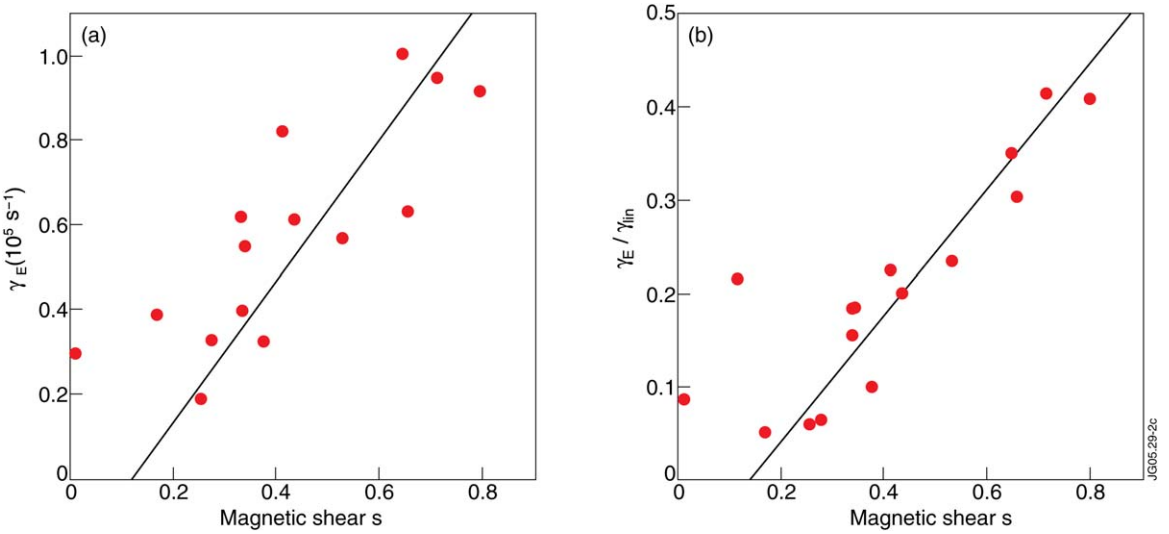

Fig. 2. (a) $E \times B$ flow shearing rate versus magnetic shear and (b) $E \times B$ flow shearing rate divided by an estimate of the ITG growth rate versus magnetic shear at the location and onset of the ITB, yielding the empirical ITB threshold condition (reproduced from [35]).

for the ITB to form. The triggering event of an ITB may be different and separate from the mechanisms that after triggering govern the physics of the ITBs, as reported in [38,39].

2.3. 1st and 2nd order transitions and consequences for power threshold

The transition types for the transport barriers (internal or edge) are traditionally classified into 1st and 2nd order transitions. 1st order transition is characterised by a sudden change of gradient, which occurs when the control parameter (usually the heat flux) crosses a threshold. On the other hand, in the 2nd order transition the temperature gradient varies continuously and there is no obvious power threshold (or heat flux threshold), for example the electron ITB forms if just the magnetic shear is negative enough even at minimal power level. In the case of 1st order transition, the threshold in the control parameter, like the heat flux, depends on local plasma parameters and thus varies from plasma to plasma, not allowing us to define for example an unambiguous universal power threshold, as discussed in Section 2.1.

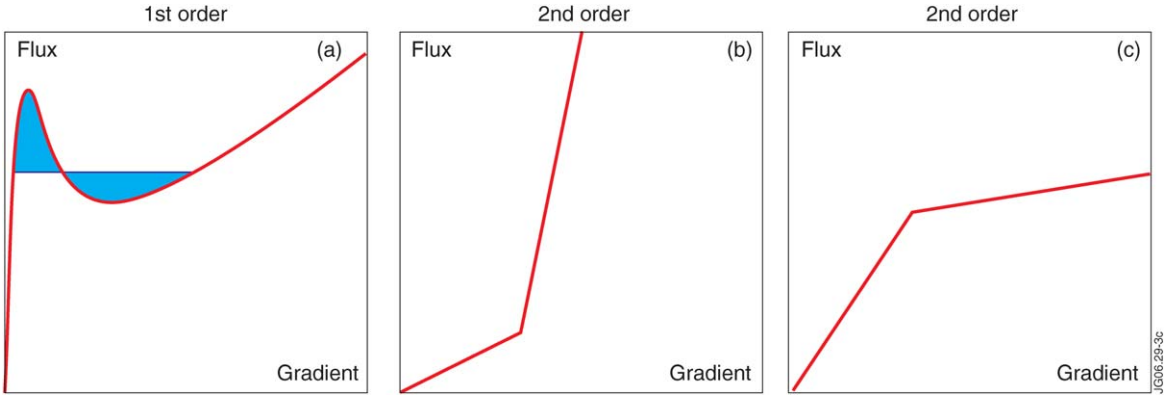

Fig. 3. (a) Schematic curve of a flux versus gradient in presence of a flow shear. The horizontal line indicates the flux that satisfies the Maxwell construction. (b) Flux versus gradient in presence of an instability threshold. A barrier may be produced by a local increase of the threshold. (c) Flattening of the flux above a critical gradient. The barrier is due to a reduction of the flux.

A 1st order transition may occur because of the reinforcement of flow shear with gradients. This is a consequence of the force balance equation, which implies that the radial electric field in a tokamak increases with the density and temperature gradients, and also with the toroidal velocity

$$E_r = \frac{\nabla p}{enZ} - v_\theta B_\varphi + v_\varphi B_\theta \tag{1}$$

where p is pressure, e the elementary charge, n density, Z the charge number, v_θ and v_ϕ, B_θ and B_ϕ the poloidal and toroidal velocities and magnetic fields, respectively. There are three contributing terms to E_r, the pressure gradient term, and the poloidal and toroidal rotation velocity terms. This link allows a positive loop where enhanced gradients lead to a larger shear rate, which in turn further improves the confinement. This positive feedback leads to a figure of the flux versus gradient that exhibits an 'S-shape' (see Fig. 3(a)). A bifurcation is therefore expected above a critical flux. It is stressed here that other mechanisms than flow shear stabilisation may lead to a 1st order transition. For instance, a positive loop may be provided by the interplay between current and pressure profiles via the current that is driven by the pressure gradient (in a tokamak, a thermoelectric effect leads to such a current, called 'bootstrap' current). Also α-stabilisation may lead to a positive feedback on the pressure gradient [40]. Finally, we note that 1st order transitions are characterised by hysteresis, i.e., different critical fluxes for the forward and back transitions.

There exist several mechanisms for explaining a 2nd order transition. One mechanism is provided by a strong increase of the instability threshold within a layer (because of combined large α and negative magnetic shear for instance), in other words a linear stabilisation of modes (see Fig. 3(b)). Non linear effects may also lead to an effective monotonic curve, which leads also to a soft transition (see Fig. 3(c)). Note also that a similar behaviour is also obtained for an S-curve when the forward and backward transitions take place at the Maxwell flux [41].

The question of 1st or 2nd order transition is quite important as it determines the existence of a power threshold, but also the barrier robustness, since hysteresis improves the barrier resilience to external perturbations. It is found that a minimum heating power is needed to trigger an ITB in JET [20]. Also impressive hysteresis effects have been observed [42]. However none of these observations demonstrate that a first order transition takes place as in both cases the current profile was found to be very different. In fact it was found that the power threshold is sometimes very low, when the current profile is optimised [43]. This latter observation indicates that if the transition is 1st order, the S-curve shown on Fig. 3 cannot be universal.

3. Experiments dedicated to understand the physics of the ITBs

3.1. Heat and cold pulse propagation across the ITBs

Electron heating power modulation experiments have been used to probe the physics of ITBs by looking into the propagation of heat pulses on JET [44]. The heat pulses are produced with modulated electron heating power by RF system. By Fourier transforming the temperature data at the modulation frequency, it is possible to obtain the

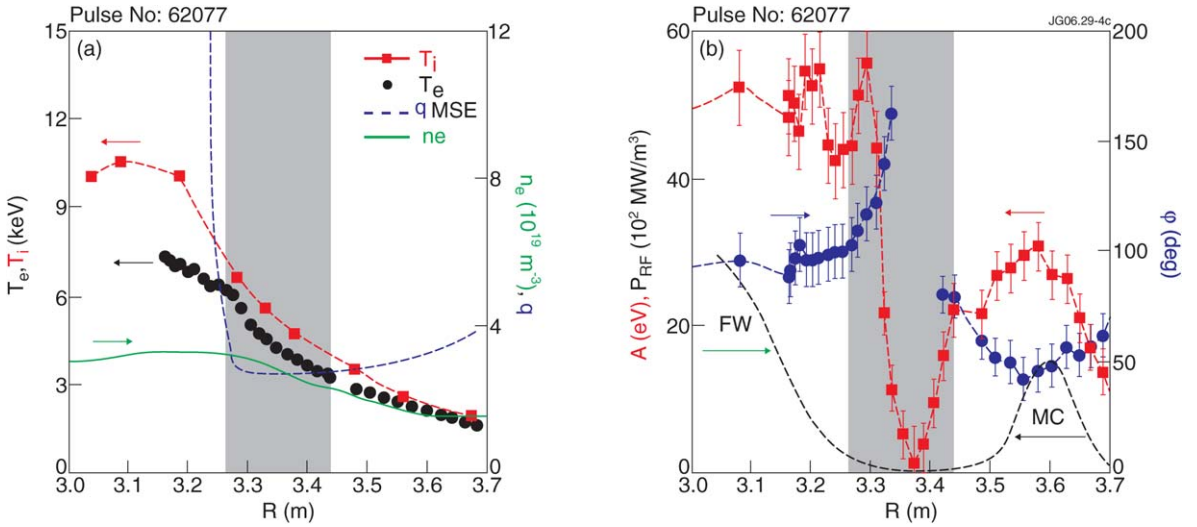

Fig. 4. (a) Experimental profiles of T_e, T_i, n_e and q for shot no. 62077 (3.25T/2.6MA, 3He ∼ 20%, ICRH $f = 37$ MHz) at $t = 5.5$ s. The ITB region is highlighted. (b) Profiles of Fourier component of A (red squares) and φ (blue circles) at the modulation frequency (20 Hz) during the time interval 5.5–5.7 s. RF power deposition profiles are also plotted (dashed black line) (reproduced from [44]). (For interpretation of the references to colour in this figure, the reader is referred to the web version of this article.)

amplitude and phase of the propagating heat wave. Two important questions can be answered with this technique [45]. The first question is related to the radial width of the barrier: is the barrier limited to a narrow layer or does it extend to the whole core region inside the barrier foot? The second question deals with the nature of the transition, i.e., whether the plasma experiences a 1st or 2nd order transition. In the case of 2nd order transition, a related question deals with the reduction of turbulence. It is recalled here that turbulence in a tokamak appears when R/L_T is larger than a threshold κ_c (R is the major radius and L_T is the temperature gradient length). It sounds reasonable to assume that this threshold becomes larger within the transport barrier due to various stabilising effects. If so, is a transport barrier a turbulent region, with R/L_T above this enhanced threshold, or is turbulence quenched because R/L_T stays below the new threshold?

The main plasma profiles as well as the amplitude A and phase φ of the heat wave are illustrated in Fig. 4. The two heat waves were produced by heating locally the plasma with radiofrequency waves. It is reminded here that $\partial_r A/A$ and $\partial_r \varphi$ roughly behave as $(\omega/\chi_e)^{1/2}$, where ω is the frequency of the heat modulation and χ_e is the electron heat diffusivity [46]. Regarding questions (1) and (2), the following conclusions can be drawn:

(1) Fig. 4 shows sharp discontinuities in the heat wave propagation (i.e., in the slopes of the A and φ profiles) both at the foot and at the top of the high ∇T_e region. This indicates that, at least for these plasma conditions, the ITB is indeed a narrow layer with a low electron heat diffusivity χ_e embedded in a higher χ_e plasma, and not a general improvement of confinement in the whole core region extending to the centre of the plasma.
(2) Fig. 4 also shows that the heat wave is strongly damped when meeting the ITB from either side. This is consistent with a situation where the turbulence is quenched because the plasma has become sub-critical with respect to a threshold value that has increased. In this case, χ_e does not depend on ∇T_e, the perturbative χ_e coincides with the power balance χ_e and is low, the two heat waves are strongly damped and cannot cross the ITB.

Another observation is that the inner slope of the amplitude A within the ITB layer is steeper than the outer ones, indicating likely a non-uniform turbulence stabilisation and reduction of the diffusivity χ_e within the ITB [44]. This is in agreement with previous experiments where the cold pulse induced at the edge showed first a growth when meeting the foot of the ITB and then strong damping further inside [47]. The growth of the cold pulse when meeting the foot of the ITB can be regarded as a strong indication in favour of the 2nd order transition as no growth would be expected in the 1st order transition [44].

3.2. Turbulence measurements in the ITB plasmas

Reflectometry is used to measure density fluctuations on JET [48]. The core and edge density fluctuations are monitored using four X-mode heterodyne reflectometer channels (at 75, 92, 96 and 105 GHz), and ten O-mode heterodyne reflectometer channels (between 18 and 69 GHz). The three main observations are as follows:

(1) the formation of a core region of high radial shear in the plasma toroidal velocity is correlated with the suppression of long wavelength turbulence $k_\perp \rho_i \ll 1$ ($k_\perp$ is the wave number perpendicular the magnetic field and is the ion Larmor radius) and with a decrease in the ion thermal conductivity χ_i in plasmas with dominant ion heating [49];
(2) the formation of an internal transport barrier is correlated with a localized suppression of shorter wavelength turbulence ($k_\perp \rho_i \sim 1$); and
(3) at least in the case of dominant electron, ITBs with no or small NBI heating resulting in no or low level of ITG turbulence, low-frequency ($f < 50$ kHz), long wave length fluctuations (dominantly TEM) are reduced for the whole region from the plasma centre out to the foot of the electron ITB [50].

The measured fluctuation levels showing clearly point (3) is illustrated in Fig. 5. In plasmas with dominant electron heating (pure or dominant electron ITBs), the turbulence reduction coincides with a region of negative shear and reduced electron thermal diffusion (calculated with the TRANSP code) as shown in Fig. 5 [50]. The analysis of turbulence measurements also suggests the dominant instabilities being TEMs, and their suppression due to negative magnetic shear leads to the formation of the ITB. This result seems to be at first sight in disagreement with the observation of the heat pulse propagating radially without any damping in the region from the centre out to the inner part of the ITB layer as discussed in Section 3.1 [44], as that was an indication of only a narrow layer of suppressed turbulence around the ITB. On the contrary, it is worth noting that in plasmas with the power modulation reported in Section 3.1, significant amount of NBI heating was used and thus, the ITG turbulence was the dominant micro-instability. Thus, turbulence stabilisation and the physics of the ITB are most probably governed by other mechanisms between the two types of plasmas/experiments. As the slab branch of the ITG is not sensitive to magnetic shear, it is

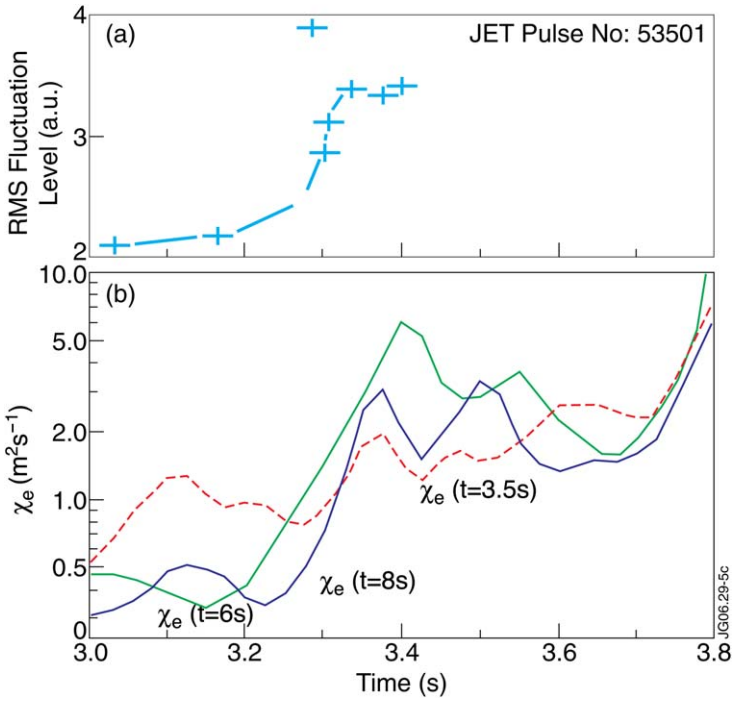

Fig. 5. (a) RMS fluctuation level profile (3–500 kHz) at $t = 8$ s, (b) electron thermal diffusivity χ_e profile from TRANSP at various times in electron ITB shot #53501 (reproduced from [50]).

possible that the heat pulse can propagate inside the ITB even with negative magnetic shear in NBI dominant plasmas where TEM and toroidal branch of the ITG are supposed to be suppressed. In addition, in the experiments with heat pulse propagation, the region inside the ITB had a current hole, and this current hole might introduce some anomalies in the behaviour of the heat pulse propagation.

4. Modelling of JET ITB plasmas

4.1. Predictive transport modelling

There are several ways to carry out predictive transport simulations of ITBs, and the conclusions based on the simulation results may depend on the simulation methodology adopted. Here we only address time dependent modelling, which challenge maximally the transport models as the whole process governing the dynamics of the ITBs.

The original Bohm/gyroBohm transport model [51] modified to include the empirical ITB threshold condition [35] (discussed in Section 2.2), has been extensively used to predict ITBs in JET. The turbulence stabilisation mechanisms to form an ITB in the Bohm/gyroBohm model are based on the combined effect of the $E \times B$ flow shear versus a simple estimate for the instability growth rate and the magnetic shear. The stabilising effect of the α-stabilisation has also been included in some simulations. This model has turned out to be the most robust model to predict the time dynamics of the ITB evolution in JET plasmas [52]. This is illustrated (dashed lines) in Fig. 6 for one JET discharge with positive magnetic shear and another one with negative magnetic shear. In spite of its heuristic nature, this model has been quite successful to understand and prepare experiments for real-time control of ITBs [53].

Also the Weiland [24] and the GLF23 transport models [54,55] have been used to predict the time evolution of the ITBs in the multi-tokamak database with the JETTO [56] and CRONOS [57] transport codes. Both transport models include qualitatively the same micro-turbulence stabilisation mechanisms, i.e., $E \times B$ flow shear, magnetic shear, α-stabilisation, dilution and density gradient effects. The predicted profiles at the end of the high performance phase for two JET discharges are illustrated in Fig. 6 [52]. The Weiland model (dash-dotted lines) does not predict a clear ITB for any of the plasma profiles although the volume averaged temperatures and density is often rather close to their

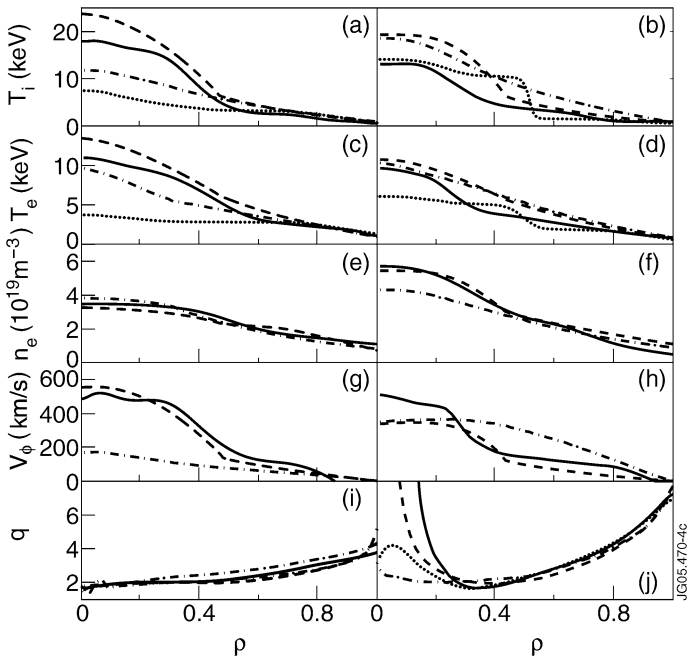

Fig. 6. Profiles of the ion temperature (a) and (b), electron temperature (c) and (d), electron density (e) and (f), toroidal rotation (g) and (h) and q (i) and (j) for JET discharges no. 46664 at $t = 6.0$ s (left-hand side) and 53521 at $t = 12.0$ s (right-hand side). The solid lines correspond to the experimental data and the dashed, dash-dotted and dotted ones to the predictions with the Bohm/GyroBohm, Weiland and GLF23 model, respectively (reproduced from [52]).

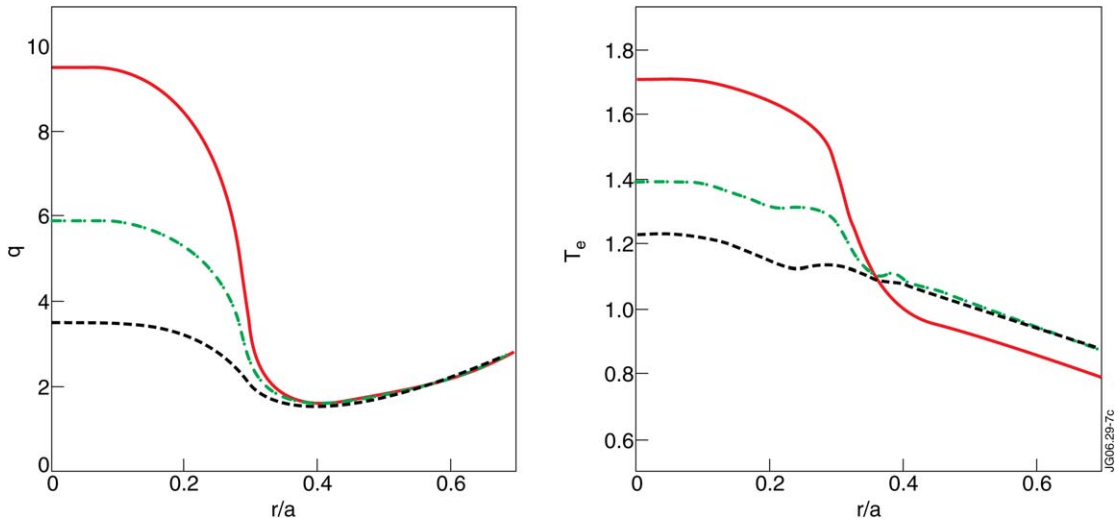

Fig. 7. Profiles of safety factor, and electron temperature calculated with the TRB turbulence code [64].

experimental values. The GLF23 transport model (dotted lines) predicts often an ITB, but not at the right location. This model tends to predict the heat transport outside the ITB more accurately than the other transport models. It is also able to predict ITBs only in one of the transport channels but not necessarily in another channel whereas, for example the Bohm/GyroBohm model always predicts an ITB in either all or no transport channels. This is a serious deficit in the Bohm/gyroBohm transport model.

4.2. Turbulence simulations of JET ITB's

The TRB and CUTIE [58] fluid codes have been used to simulate ITBs in JET. TRB [59,60] is a full torus, electrostatic, fixed flux code solving fluid equations for ITG and trapped electron modes (TEM). The evolution of electron density and pressure, vorticity, parallel ion velocity and ion pressure is computed, whereas the q-profile is frozen. CUTIE is a global electromagnetic fluid turbulence code. It solves the evolution equations for the fluctuating electron density, electron and ion temperatures, velocity, potential and magnetic field.

Ion ITBs are found with the TRB code. Stability comes from a mixture of stabilisation via negative magnetic shear and rarefaction of resonant surfaces (in particular close to a safety factor that is a low order rational number). This 'gap' in the density of resonant surfaces is wider when $q_{\min}$ is close to a low order rational number. Also several gaps may appear simultaneously, leading to multiple barriers. However, these features were not recovered in recent gyrokinetic simulations with the GYRO code, which indicate that non resonant modes fill the gap [13]. The CUTIE code also finds that rational values of $q_{\min}$ are important [61]. This comes from a turbulent dynamo effect, which modifies the local magnetic shear, and a localised velocity shear generated by turbulence. This mechanism is difficult to verify experimentally, although large transients in the $E \times B$ flow were observed in TFTR [62] and on JET [63].

ITBs in the electron transport channel are also found by the TRB code [64]. They appear to be triggered mainly by negative magnetic shear, as shown on Fig. 7. This effect is amplified for values of $\alpha = -q^2 R\, \mathrm{d}\beta/\mathrm{d}r$ of the order of unity. For electron modes, theory predicts stability when $s < 3\alpha/5 - 3/8$ [65]. Also electron ITBs appear at the minimum of safety factor, if the gap width in the density of rational surfaces is large enough (with the caveats already mentioned concerning the role of non-resonant modes).

5. Conclusions

This article is a summary of the studies carried out in JET to understand the physics of ITBs. There are several open questions related to the physics of the ITBs to which these studies aim at giving answers. The main open issues are listed below and also discussed in a recent paper [66]:

(1) Which are dominant mechanisms for ITB formation? Does the onset of an ITB have a characteristic of a 1st or 2nd order transition?
(2) What is the role of the integer and rational surfaces of the q-profile?
(3) How is the turbulence reduced? Does the suppression of turbulence extend radially from the footpoint of the ITB up to the centre of the plasma or is limited to a narrow layer around the ITB?
(4) Why do the theory-based transport models struggle in predicting the time dynamics of the ITBs?

Regarding the question of dominant mechanisms, many experimental results in JET are consistent with a barrier dynamics controlled by flow shear and local magnetic shear (in a broad sense, i.e., including α stabilisation). These results also indicate that the onset of an ITB is highly sensitive to the profile of the safety factor (q-profile). The level of $E \times B$ velocity shear rate that is needed to form a barrier decreases when the local magnetic shear becomes smaller. Part of these observations can be explained by the parametric dependences of the linear growth rate, and are qualitatively consistent with turbulence simulations. Regarding the relative weights of shear flow and magnetic shear when a barrier is triggered, pure electron ITBs provide useful information. They usually develop in regions where the magnetic shear is negative. Also neoclassical theory predicts that the $E \times B$ velocity shear is small in this case, since the density and ion temperature gradients are small, and there is no external source of toroidal momentum. Hence it can be safely said that the current profile plays a major role in the formation of electron ITBs. The situation is less clear for ion transport barriers. Many ion ITBs in JET appear at zero magnetic shear and low order rational $q_{\min}$. Ion barriers may develop with RF heating only, i.e., without an external source of toroidal momentum. Finally the level of $E \times B$ velocity shear rate that is needed to trigger a barrier decreases when the local magnetic shear becomes smaller (when $s < 1$). These observations suggest that a strong $E \times B$ velocity shear rate is not mandatory for ITB formation, provided the q-profile is appropriate. This conclusion must be softened by the fact that diamagnetic flow shear is never negligible when an ion barrier builds up. Hence it cannot be fully ascertained that an optimised q-profile alone is sufficient for barrier formation. The ITB on the toroidal momentum transport channel appears simultaneously with the ion ITB and thus, the turbulence stabilisation mechanism is supposed to be the same as for the ion heat transport channel.

The interplay between flow shear and magnetic shear is also related to the question of the transition order. Regarding this issue, progress has been made thanks to the analysis of cold pulse propagation across ITBs. The amplification of the thermal wave that is observed at the ITB is consistent with a second order rather than first order transition.

An explanation based on a combination of flow shear and magnetic shear is unable to explain the full range of barriers observed in JET. There are two reasons at least for this statement: the role of integer values of q in positive magnetic shear, the role of low order rational value of the minimum safety factor $q_{\min}$ and the coexistence of several barriers. The favourable role of 'rational $q_{\min}$' has been confirmed thanks to the observation of MHD activity (Alfvén wave cascades, which appear only if $q_{\min}$ is rational), correlated with the onset of the barrier. Also a transition is often observed between a single barrier localised at negative shear and a double barrier, when $q_{\min}$ crosses a low order rational number. In fact, the trigger mechanism of the ITB (for example integer value of q) seems to be often different from the mechanisms governing the physics and dynamics of the ITB later on (for example $E \times B$ velocity shear, magnetic shear, α-stabilisation, etc.).

The issue of the barrier location and width is obviously crucial for the extrapolation to a next step device. Heat modulation experiments indicate that transport barriers have a finite width, i.e., do not extend up to the magnetic axis. This observation may look to be in contrast with density fluctuation measurements done with reflectometry, which indicate a reduction of turbulence in the whole region located between the magnetic axis and the foot of the ITB. However, it is possible that both observations are possible, as the experimental conditions were different. Hence this question will require further investigation.

Finally, the results for predictive modelling are contrasted. Although semi-heuristic transport models have been proved to simulate JET discharges with a fair degree of accuracy, theory based models often fail to predict the barrier formation at the right time. When the barrier formation is correctly predicted, the location and/or the shape of the ITB are sometimes poorly reproduced. There are at least two reasons for this poor predictive capability. First most transport models do not encompass a particular role of rational surfaces, which is known to be important from experiment. Second they usually assume that the poloidal flow is consistent with conventional collisional models, whereas anomalous values have been observed on TFTR and JET. Thus the improvement of transport models certainly remains a key issue and a challenge for future developments.

Acknowledgements

This work has been conducted under the European Fusion Development Agreement.

References

[1] Y. Koide, M. Kikuchi, M. Mori, et al., Phys. Rev. Lett. 72 (1994) 3662.
[2] G.T. Hoang, et al., Nucl. Fusion 34 (1994) 75.
[3] F. Levinton, M. Zarnstoff, S. Batha, et al., Phys. Rev. Lett. 75 (1995) 4417.
[4] E. Strait, L. Lao, M. Mauel, et al., Phys. Rev. Lett. 75 (1995) 4421.
[5] JET Team, C. Gormezano, in: Proc. 16th Int. Conf., Montreal, 1996, in: Plasma Physics and Controlled Nuclear Fusion Research, vol. 1, IAEA, Vienna, 1997, p. 487.
[6] O. Gruber, et al., Plasma Phys. Control. Fusion 42 (2000) A117.
[7] R.C. Wolf, Plasma Phys. Control. Fusion 45 (2003) R1.
[8] J.W. Connor, T. Fukuda, X. Garbet, et al., Nucl. Fusion 44 (2004) R1.
[9] J.F. Drake, Y.T. Lau, P.N. Guzdar, et al., Phys. Rev. Lett. 77 (1996) 494.
[10] J.E. Kinsey, G.M. Staebler, K.H. Burrell, M.E. Austin, R.E. Waltz, Phys. Rev. Lett. 86 (2001) 814.
[11] F. Romanelli, F. Zonca, Phys. Fluids B 5 (1993) 4081.
[12] J.W. Connor, R.J. Hastie, Phys. Rev. Lett. 92 (2004) 075001.
[13] J. Candy, R. Waltz, M.N. Rosenbluth, Phys. Plasmas 9 (2004) 1938.
[14] R.E. Waltz, G.D. Kerbel, J. Milovitch, G.W. Hammett, Phys. Plasmas 2 (1995) 2408.
[15] H. Biglari, P. Diamond, P.W. Terry, Phys. Fluids B 2 (1990) 1.
[16] T.S. Hahm, K.H. Burrell, Phys. Plasmas 2 (1995) 1648.
[17] G. Tresset, X. Litaudon, D. Moreau, et al., Nucl. Fusion 42 (2002) 520.
[18] R.C. Wolf, et al., Plasma Phys. Control. Fusion 45 (2003) 1757.
[19] C.D. Challis, et al., Plasma Phys. Control. Fusion 44 (2002) 1031.
[20] C.D. Challis, et al., Plasma Phys. Control. Fusion 43 (2001) 861.
[21] E. Joffrin, et al., Plasma Phys. Control. Fusion 44 (2002) 1739.
[22] S.E. Sharapov, et al., Alfven cascades in JET discharges with NBI heating, Nucl. Fusion (2006), in press.
[23] M.E. Austin et al., in: 47th APS-DPP Meeting Denver, Colorado, 2005.
[24] J. Weiland, Collective Modes in Inhomogeneous Plasmas, IOP, 2000.
[25] A.L. Rogister, Nucl. Fusion 41 (2001) 1101.
[26] C. Bourdelle, et al., Nucl. Fusion 42 (2002) 892.
[27] M. Kotschenreuther, W. Dorland, M.A. Beer, et al., Phys. Plasmas 2 (1995) 2381.
[28] R.V. Budny, R. Andre, A. Becoulet, et al., Plasma Phys. Control. Fusion 44 (2002) 1215.
[29] F. Crisanti, B. Esposito, C. Gormezano, et al., Nucl. Fusion 41 (2001) 883.
[30] L.-G. Eriksson, C. Fourment, V. Fuchs, et al., Phys. Rev. Lett. 88 (2002) 145001.
[31] D.E. Newman, B.A. Carreras, D. Lopez-Bruna, et al., Phys. Plasmas 5 (1998) 938.
[32] W.A. Houlberg, K.C. Shaing, S.P. Hirshman, M.C. Zarnstorff, Phys. Plasmas 4 (1997) 3230.
[33] J. Kim, et al., Phys. Rev. Lett. 72 (1994) 2199.
[34] X. Garbet, Y. Baranov, G. Bateman, et al., Nucl. Fusion 43 (2003) 975.
[35] T.J.J. Tala, J.A. Heikkinen, V.V. Parail, et al., Plasma Phys. Control. Fusion 43 (2001) 507.
[36] P. Maget, B. Esposito, E. Joffrin, et al., Plasma Phys. Control. Fusion 45 (2003) 1385.
[37] B. Esposito, F. Crisanti, V. Parail, et al., Plasma Phys. Control. Fusion 45 (2003) 933.
[38] E. Joffrin, C.D. Challis, T.C. Hender, et al., Nucl. Fusion 42 (2002) 235.
[39] E. Joffrin, C.D. Challis, G.D. Conway, et al., Nucl. Fusion 43 (2003) 1167.
[40] C. Bourdelle, G.T. Hoang, X. Litaudon, C.M. Roach, T. Tala, for the ITPA Topical Group on Transport and ITB Physics, the International ITB Database Working Group, Nucl. Fusion 45 (2005) 110.
[41] S.-I. Itoh, K. Itoh, S. Toda, Phys. Rev. Lett. 89 (2002) 215001.
[42] Yu.F. Baranov, C. Bourdelle, T. Bolzonella, et al., Plasma Phys. Control. Fusion 47 (2005) 975.
[43] A. Becoulet, Plasma Phys. Control. Fusion 43 (2001) A395.
[44] P. Mantica, et al., Phys. Rev. Lett. 96 (2006) 95002.
[45] X. Garbet, P. Mantica, F. Ryter, et al., Plasma Phys. Control. Fusion 46 (2004) 1351.
[46] P. Mantica, F. Ryter, Perturbative studies of turbulent transport in fusion plasmas, C. R. Physique 7 (2006), this volume.
[47] P. Mantica, G. Gorini, F. Imbeaux, et al., Plasma Phys. Control. Fusion 44 (2002) 2185.
[48] G. Conway, G. Vayakis, J.A. Fessey, D.V. Bartlett, Rev. Sci. Instrum. 70 (1999) 3921.
[49] G.D. Conway, D.N. Borba, B. Alper, et al., Phys. Rev. Lett. 84 (2000) 1463.
[50] G.D. Conway, G.M.D. Hogeweij, M.R. de Baar, et al., Plasma Phys. Control. Fusion 44 (2002) 1167.
[51] M. Erba, A. Cherubini, V.V. Parail, et al., Plasma Phys. Control. Fusion 39 (1997) 261.
[52] T. Tala, F. Imbeaux, V. Parail, et al., Nucl. Fusion 46 (2006) 548.
[53] T. Tala, L. Laborde, D. Mazon, et al., Nucl. Fusion 45 (2005) 1027.

[54] R.E. Waltz, M. Staebler, W. Dorland, et al., Phys. Plasmas 4 (1997) 2482.
[55] J.E. Kinsey, G.M. Staebler, R.E. Waltz, Phys. Plasmas 12 (2005) 052503.
[56] G. Genacchi, A. Taroni, JETTO: A free boundary plasma transport code (basic version), Rapporto ENEA RT/TIB 1988(5).
[57] V. Basiuk, J.F. Artaud, F. Imbeaux, Nucl. Fusion 43 (2003) 822.
[58] A. Thyagaraja, Plasma Phys. Control. Fusion 42 (2000) B255.
[59] X. Garbet, C. Bourdelle, G.T. Hoang, et al., Phys. Plasmas 8 (2001) 2793.
[60] I. Voitsekhovitch, X. Garbet, S. Benkadda, et al., Phys. Plasmas 9 (2002) 4671.
[61] A. Thyagaraja, P.J. Knight, N. Loureiro, Europ. J. Mech. B/Fluids 23 (2004) 475.
[62] R.E. Bell, et al., Phys. Rev. Lett. 81 (1998) 1429.
[63] K. Crombé, et al., Phys. Rev. Lett. 95 (2005) 155003.
[64] Y. Baranov, et al., Plasma Phys. Control. Fusion 46 (2004) 1181.
[65] P. Maget, X. Garbet, A. Géraud, E. Joffrin, Nucl. Fusion 39 (1999) 949.
[66] X. Litaudon, Plasma Phys. Control. Fusion 48 (2006) A1.